DALTON
FULL PAPER

Kinetics and mechanisms of the complexation of aqueous lanthanide ions by 4-(2-pyridylazo)resorcinol †

Yanlong Shi,[a] Edward M. Eyring *[a] and Rudi van Eldik *[b]

[a] *Department of Chemistry, University of Utah, Salt Lake City, Utah 84112, USA*
[b] *Institute for Inorganic Chemistry, University of Erlangen-Nürnberg, 91058 Erlangen, Germany*

Received 24th July 1998, Accepted 14th August 1998

Three kinetic steps were observed for the complexations of Eu^{3+} and UO_2^{2+} by PAR [4-(2-pyridylazo)resorcinol] or PAN [1-(2-pyridylazo)-2-naphthol] in different buffered solutions. The first step can be assigned to the co-ordination of the nitrogen donor from the pyridine moiety of the ligand based on the dependencies of [Eu^{3+}], pH, pressure, nature and concentration of the buffer. The rate-determining step is the release of water molecules from the co-ordination sphere of the lanthanide ion. Variations in the rate of the first step with different lanthanide ions indicated that a co-ordination number changeover is involved in this lanthanide series. For the second step the formation of a "hydroazone–Ln^{3+} chelate" intermediate accounts for all of the observed kinetic behaviors. The kinetic investigations of the third step show that there is a deprotonation preequilibrium preceding the transition state of the final product with two chelated 5-membered rings involved. Surprisingly, the rate constants of the three steps for the complexation of UO_2^{2+} by PAR are very close to those for 18-crown-6 and diaza-18-crown-6 reacting with uranyl ion. The differences in the kinetics between PAR and PAN can be related to the difference in their structures.

The fifteen trivalent lanthanide, or f-block, ions ranging from La^3 to Lu^{3+} represent the most extended series of chemically similar metal ions. The progressive filling of the 4f orbitals from La^{3+} to Lu^{3+} is accompanied by a smooth decrease in the cation radius r_M with increasing atomic number because of the increasingly strong nuclear attraction for the electrons in the diffuse f orbitals (the lanthanide contraction). In an ideal situation, smooth variation of rate parameters with radii might be expected. However, the solution chemistry of the lanthanides displays more interesting variation than a simple linear correlation of rate and/or thermodynamic parameters with shrinking cation radius.[1,2] A changeover in the co-ordination number of the lanthanide complexes from nine to eight near the middle of the series[3–6] gives rise to kinetics for the complexation or solvent exchange of lanthanide ions in solution that has been studied extensively using high-pressure NMR relaxation techniques.[7–13] Interest in these kinetic phenomena has increased with the development of some lanthanide complexes as contrast agents in magnetic imaging (MRI).[14–16] Another significant feature of lanthanide element behavior in aqueous solution is the very high stability of the trivalent state although cerium(IV) and, in strongly reducing solutions, divalent samarium, europium and ytterbium can be formed.[17,18] A third important characteristic is the strongly ionic character of lanthanide bonding. Thus, the lanthanides are typically "hard acids".

The kinetics of complexation is normally quite fast for Ln^{3+} cations reacting with simple ligands compared to the rates of complexation for analogous complexes of the transition metal ions in the same oxidation state. The kinetics of complexation of Ln^{3+}(aq) by many monodentate or multidentate ligands has been studied using fast kinetic techniques. The ligands include NO_3^- (ultrasonic relaxation),[19,20] SO_4^{2-} (ultrasonic relaxation),[21,22] acetate (ultrasonic relaxation),[23] picolinic acid (pyridine-2-carboxylic acid) (pulse-radiolytic pH-jump),[24] murexide (E-jump),[25] methyl red (pulse-radiolytic pH-jump),[26] anthranilate (temperature-jump),[26] malonate (ultrasonic relaxation),[27] oxalate (pressure-jump),[28] arsenazo III [3,6-bis-(*o*-arsonophenylazo)-4,5-dihydroxynaphthalene-2,7-disulfonic acid] (stopped-flow)[13] and acyclic aminopolycarboxylates, such as EDTA (ethylenedinitrilotetraacetate) and DTPA [carboxymethyliminobis(ethylenenitrilo)tetraacetate].[18,29] The rate of complexation is affected either by the size of the central ion or by the nature of the ligand. However, the complexations of Ln^{3+} by cyclic aminopolycarboxylates, such as DOTA (1,4,7,10-tetraazacyclododecane-*N*,*N*′,*N*″,*N*‴-tetraacetic acid), are slower and susceptible to study by traditional UV/VIS spectrophotometric techniques.[18,30–39] The rate-determining step of the complexation of Ln^{3+} by cyclic aminocarboxylates is proton loss from the ligand and the rearrangement of the intermediate. The rate of complexation is also affected by the ring size of the ligands.

The well known analytical reagents PAR [4-(2-pyridylazo)resorcinol] and PAN [1-(2-pyridylazo)-2-naphthol], like arsenazo III, have been studied extensively for the colorimetric determination of lanthanides and uranium(VI)[40] since they form stable, intensely colored complexes with a molar absorptivity of $(3–8) \times 10^4$ M^{-1} cm^{-1}. The compound PAR has been used widely in analytical chemistry because both it and the lanthanides and uranium(VI) complexes are water soluble, thus simplifying the analysis since no expensive, or toxic, organic solvents are required.

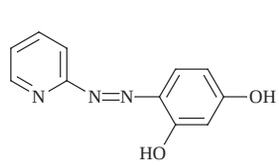

PAR

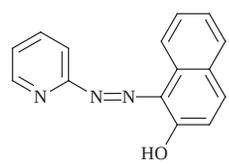

PAN

Although the IR spectra,[41,42] Raman spectra,[43] acid–base equilibria[44,45] and HMO (Hückel molecular orbital) quantum calculations[45] of PAR and PAN, and some structural chemistry[46–49] and stability constants[50–52] of their lanthanide complexes have been investigated, neither bonding information

† *Supplementary data available*: rate constants as a function of buffer concentration for the Eu^{3+}–PAR reaction. For direct electronic access see http://www.rsc.org/suppdata/dt/1998/3565/, otherwise available from BLDSC (No. SUP 57431, 2 pp.) or the RSC Library. See Instructions for Authors, 1998, Issue 1 (http://www.rsc.org/dalton).

between the lanthanide ion and the ligand nor kinetic studies have been reported for the complexation of lanthanides by PAR and PAN. However, some kinetics of the complexation of transition metal ions by PAR and PAN has been reported.[53–66] Differences between transition metal ions and lanthanide or actinide ions make it interesting to study the complexation kinetics of lanthanide ions and uranium(VI) with PAR and PAN.

We have sought a clear understanding of the nature of the different contributions to the complexation kinetics and mechanism (*e.g.*, ligand geometry, size of the central metal ion, pH, buffer, pressure, *etc*.). In the present paper, we mainly focus on the complexation of Eu^{3+} by PAR and PAN, under different buffer environments in the pH range of 1.8–8.1 using either conventional or high-pressure stopped-flow spectrophotometric techniques. In addition, we also studied the kinetics and mechanism of the complexation of other lanthanide(III) ions and UO_2^{2+} by PAR for comparison.

Experimental

Materials

The compounds PAR, PAN and Sudan Orange G [4-(phenylazo)resorcinol] were obtained from Aldrich and recrystallized from methanol, $LaCl_3·6H_2O$, $CeCl_3·7H_2O$, $PrCl_3·6H_2O$, $NdCl_3·6H_2O$, $SmCl_3·6H_2O$ and $DyCl_3·6H_2O$ from Aldrich, $EuCl_3·6H_2O$, $GdCl_3·6H_2O$, $ErCl_3·6H_2O$, $YbCl_3·6H_2O$ and $LuCl_3·6H_2O$ from Strem and $TbCl_3·6H_2O$ from Alfa. All these lanthanides were used as received (purity >99.9%); $HoCl_3·6H_2O$ and $YbCl_3·6H_2O$ were prepared from Ho_2O_3 (Strem) and Yb_2O_3 (Sigma) and $UO_2(ClO_4)_2·6H_2O$ (Alfa) was used as received. *N*′-2-Hydroxyethylpiperazine-*N*-3-propanesulfonic acid (HEPPS), MES [2-(morpholino)ethanesulfonic acid] and Tris [tris-(hydroxymethyl)aminomethane] were obtained from ICN Biochemicals. Imidazole (Eastman Kodak) was recrystallized from benzene. Succinic acid, sodium salt (A. R.) was from Aldrich. Acetate buffer solution was prepared by treating acetic acid (J. T. Baker) with sodium hydroxide. Succinate buffer solution was made by mixing succinic acid dipotassium salt (Eastman Kodak) with perchloric acid (Fisher Scientific). The pH of HEPPS, MES and Tris buffer solutions was adjusted with NaOH. Distilled water was purified using a Barnstead "E-Pure" purification system. 1,4-Dioxane (spectrophotometric grade) was from Aldrich. Stock solutions of the lanthanides and ligands were prepared by weight; $NaClO_4$ (Aldrich) was used to maintain the ionic strength.

All glassware was first treated with an EDTA solution and then cleaned with successive detergent, ammonia, and distilled water rinses. The pH was adjusted by adding $HClO_4$ (Fisher Scientific, ACS reagent) or NaOH solutions (Aldrich).

Instrumentation

Spectrophotometric measurements were made with a Hewlett-Packard 8452A diode array spectrophotometer equipped with a thermostatted cell holder. pH-Metric measurements were made with an Orion Research 701 A Digital Ionanalyzer equipped with glass and calomel combined electrodes.

Kinetic studies

Kinetic measurements were made either at atmospheric pressure on a Durrum stopped-flow spectrophotometer or on a home-made, high pressure stopped-flow system[67] for pressures up to 1000 bar. n-Heptane was used as the pressurizing medium. An Edmund Scientific f/3.9 monochromator (1 nm per division) and a Hamamatsu photomultiplier tube (R376) were employed in all kinetic measurements. Transmitted light intensity *versus* time signals were recorded on a Tektronix (model 7D20) storage oscilloscope and transferred to a PC, on which data were fitted with the On Line Instrument System (OLIS) KINFIT (Bogart, GA) programs. Several experimental traces were averaged in the determination of each rate constant. The complexation of Ln^{3+} or UO_2^{2+} by PAR or PAN was studied at 25 °C. Constant temperature was maintained with a Forma Scientific model 2006 constant temperature bath and circulator system for the ambient Durrum D-110 Stopped-Flow Spectrophotometer, and a Brinkmann Instrument Lauda K-2/RD constant temperature apparatus for the high-pressure stopped-flow spectrophotometer at 25.0 °C. Temperature control precision was ±0.1 °C. All kinetic data were measured after not less than 1 h of temperature equilibriation.

Experimental rate constants reported in the Results section are the average of at least 5 replicate determinations. The optimum observation wavelength of 502 nm was determined from preliminary observations on a HP 8452A spectrophotometer.

Calculations

All experimental runs for the three consecutive kinetic steps were best described by a single exponential. Observed pseudo-first-order rate constants were obtained from a least-squares fit of at least 3 half-lives of the reactions. Volumes of activation were obtained by a fit of the natural logarithm of the observed pseudo-first-order rate constants using eqn. (1). Here k_0 denotes

$$\ln k = \ln k_0 - (\Delta V^{\ddagger} P/RT) \qquad (1)$$

the rate constant at ambient pressure. Errors reported in the Tables correspond to one standard deviation.

Results and discussion

Structure, acid–base equilibria and tautomeric equilibria of PAR

The visible spectra of 4-(2-pyridylazo)resorcinol were studied by Geary *et al.*[44] as a function of pH from 1.0 to 13.0 and the chromophoric species were identified as follows: protonated form (A), $\lambda_{max} = 420$ nm, $\varepsilon = 14\,750$ dm^3 mol^{-1} cm^{-1}, pH 1.06 and 1.52; free base form (B), $\lambda_{max} = 392$ nm, $\varepsilon = 15\,240$ dm^3 mol^{-1} cm^{-1}, pH 3.19, 4.35 and 5.56; monoionic form (C), $\lambda_{max} = 414$ nm, $\varepsilon = 23\,100$ dm^3 mol^{-1} cm^{-1}, pH 7.56–13.56; diionic form (D), $\lambda_{max} = 502$ nm, $\varepsilon = 17\,800$ dm^3 mol^{-1} cm^{-1}, pH 12.96 and 13.56. The relationship among all the species is summarized in Scheme 1.

Zhao *et al.*[45] suggested that there are five forms for PAR in aqueous alcohol solution. The equilibria are: $H_4L^{2+} \underset{K_{a1}}{\overset{-H^+}{\rightleftharpoons}} H_3L^+ \underset{K_{a2}}{\overset{-H^+}{\rightleftharpoons}} H_2L \underset{K_{a3}}{\overset{-H^+}{\rightleftharpoons}} HL^- \underset{K_{a4}}{\overset{-H^+}{\rightleftharpoons}} L^{2-}$. The p$K_a$ values are pK_{a1} = −2.30, pK_{a2} = 3.00, pK_{a3} = 5.58 and pK_{a4} = 12.03, respectively. They found that the H_3L^+ is present in a hydrazone form (see Scheme 1); H_2L exists in both the hydrazone and azo forms. The results[45] are in agreement with those obtained by Drozdzewski[43] from resonance Raman spectra. The anions HL^- and L^{2-} exist in the azo forms, and are consistent with the result of Geary *et al.* shown in Scheme 1.

Bonding and stability constants of the Ln^{III}–PAR complexes

When a 1×10^{-4} mol dm^{-3} PAR solution is mixed with a 1×10^{-3} mol dm^{-3} Eu^{3+} solution at pH 4.35 in 0.1 mol dm^{-3} acetate buffer using a tandem cuvette the λ_{max} immediately shifts from 390 to 502 nm. This indicates that complexation of Eu^{3+} (aq) by PAR does take place and raises the question what the structure of the formed complex could be.

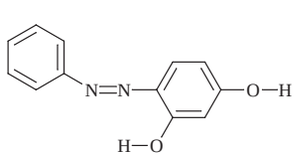

Sudan Orange G

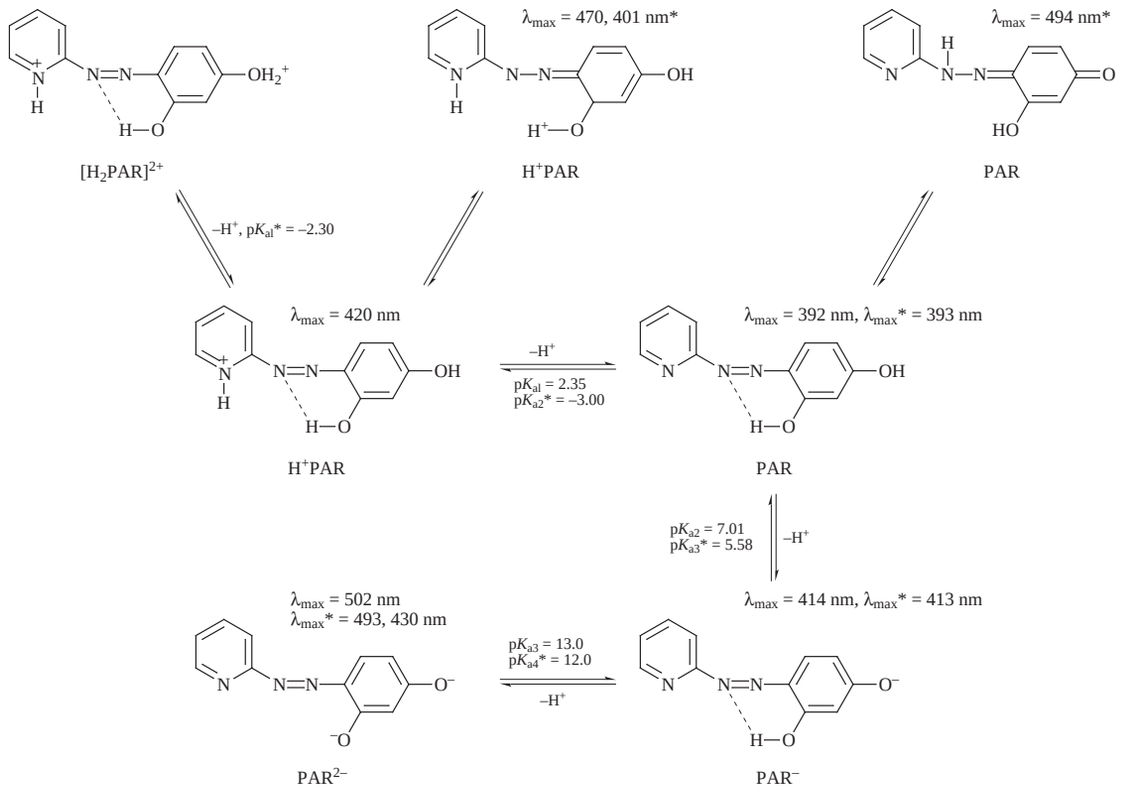

Scheme 1 λ_{max} and pK_a values, measured in water solution, cited from ref. 44; λ_{max}* and pK_a* values, measured in water–alcohol solution, cited from ref. 45.

In order to study the bonding between PAR and Eu^{3+}, we used Sudan Orange G to react with Eu^{3+} as a function of pH. We found that the metal complex absorbed at almost the same wavelength as the ligand itself at different pH values below 7. For example, when [Sudan Orange G] = 1×10^{-4} mol dm^{-3} at pH 5.4 in 0.05 mol dm^{-3} acetate buffer λ_{max} is 374 nm for free Sudan Orange G, and λ_{max} is still at 374 nm after mixing with aqueous 1×10^{-3} mol dm^{-3} Eu^{3+} solution (1 : 1 v/v). The role of the pyridine nitrogen atom of PAR in the colorimetric reaction with Eu^{3+} ion is evident from these results. The fact that there is no shift in λ_{max} on chelation by the benzene analogue of PAR, Sudan Orange G, must mean that the nitrogen atom from the pyridine moiety of PAR is involved in the bonding to Eu^{3+}.

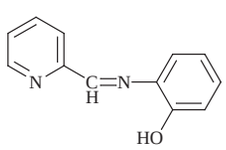

2-(*o*-hydroxyphenyliminomethyl)pyridine

To test which one of the nitrogen atoms of the azo group participates in the bonding, Geary *et al.*[44] found that when the copper(II) ion reacts with 2-(*o*-hydroxyphenyliminomethyl)-pyridine, the complex absorbs at a wavelength of 395 nm at pH values above 8.50. This represents a shift of 15 nm away from the maximum wavelength of the ligand at this pH. This shift is considerably less than the shift for the copper or europium complexes of PAR, yet the co-ordinating system is the same as in the PAR system except that the azo nitrogen nearest the heterocycle is replaced by a CH= group. The removal of this nitrogen has a profound effect on the color reaction with metal ions, and it seems clear that in PAR the azo nitrogen farthest from the heterocycle must play a greater role in the chromophoric reaction than its neighbors.

This conclusion is further supported by the visible spectra of the metal complexes of 2-(salicyclideneamino)pyridine.[44] This ligand gave strongly absorbing red complexes of transition

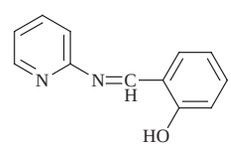

2-salicylideneaminopyridine

metal ions similar to those with PAR. For example, the main peak of the ligand at 350 nm at pH 4.88 is shifted to 453 nm at this pH in the presence of copper(II).

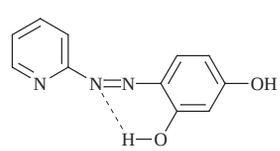

PAR with "intramolecular hydrogen bonding"

These results demonstrate that in the Eu^{3+}–PAR complex the chromophoric reaction is due to co-ordination by the pyridine nitrogen, the azo nitrogen farthest from the heterocycle, and the *o*-hydroxyl group, even though there is an "intramolecular hydrogen bonding" as shown in free PAR. The partial co-ordination of Eu^{3+}(aq) by PAR can decrease the pK_a values for the deprotonation of both the *o*- and the *p*-hydroxyl groups, and therefore the deprotonation takes place at much lower pH. The sensitivity of the color reaction of this ligand with metal ions is therefore explained by the combination of a pseudo-phenanthroline system and *o*,*o*′-disubstituted azo dyestuff.

The stability constants of Ln^{3+}–PAR have been measured by Ohyoshi[51,52] using UV/VIS spectrophotometry. Both Ln^{3+}–PAR^- and Ln^{3+}–PAR^{2-} complexes form in the pH range 5–6. The stability constants, log K (Ln^{3+}–PAR^-) and log K (Ln^{3+}–PAR^{2-}), range from 3.78 ± 0.02 (Ce) to 4.39 ± 0.02 (Lu), and from 9.61 ± 0.06 (Ce) to 10.70 ± 0.05 (Lu), respectively. The acidity of the Ln^{3+}–PAR^- complexes parallels the order of stability of the Ln^{3+}–PAR^{2-} complexes.

In an attempt to elucidate the co-ordination structure of the

PAR complexes, extraction studies of the 1:2 Ni–PAR complexes were carried out by Hoshino *et al.*[68] They suggested that in the chelation of $Ni(PAR^-)_2\cdot 2H_2O$ and $[Ni(PAR^{2-})_2]^{2-}$ the PAR^- and PAR^{2-} are acting as bidentate and terdentate ligands, respectively. They suggested that the basic change in the chelate structure from $Ni(PAR^-)_2\cdot 2H_2O$ to $[Ni(PAR^{2-})_2]^{2-}$ and deprotonation of the PAR^- ligand both cause a substantial increase in the absorptivity (from 3.73×10^4 to 8.08×10^4 dm^3 mol^{-1} cm^{-1}). Although the 1:1 lanthanide–PAR complexes differ in type from the Ni–PAR complexes, a considerable increase in the absorptivity [from $(0.95–1.15) \times 10^4$ to 3.0×10^4 dm^3 mol^{-1} cm^{-1}] was similarly observed with increasing pH. The Ln^{3+}–PAR^{2-} complexes may have a more stable chelate structure which gives rise to a larger difference in stability than for the Ln^{3+}–PAR^- complexes.

Based on all the information given above it appears that the structures of the 1:1 Eu^{3+}–PAR^- and Eu^{3+}–PAR^{2-} complexes are those shown below.

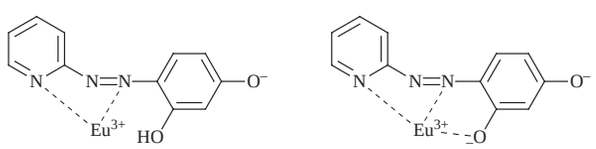

1:1 Eu^{3+}-PAR^-complex 1:1 Eu^{3+}-PAR^{2-}complex

Overview of the observed kinetics

All kinetic runs were made with at least a 10-fold excess of Eu^{3+}. The reaction of aqueous Eu^{3+} with PAR occurs in two steps in succinate buffered solution when pH < 2.65. Three steps were observed at 502 nm on different timescales when pH > 2.65. The first is much faster than the second and third with a half-life of 2 ms to 100 s, depending upon pH, Eu^{3+} concentration, amine buffer concentration, the nature of the amine buffer, pressure, and the nature of the lanthanide ions and UO_2^{2+}. A typical kinetic trace is shown in Fig. 1(a). The first step is assigned to the complexation of Eu^{3+}(aq) by the nitrogen atom from pyridine since the kinetics traces could be obtained when the pH was as low as 1.80 at a rate which depended on the pH. Fig. 1(b) is a typical kinetic trace for the second step showing that the absorbance at 502 nm decreases with increasing time with a half-life of *ca.* 500 ms. The second step is independent of pH, Eu^{3+} concentration, amine buffer concentration, the nature of the amine buffer and the choice of the lanthanide ions, but the rate increases with increasing pressure. We assign the second step to the formation of the "hydrazone–Eu^{3+} chelate" intermediate of a "phenanthroline style". In the third slowest step the absorbance at 502 nm increases with increasing time. A typical kinetic trace for this step at pH 7.55 in HEPPS buffer solution is shown in Fig. 1(c). The third step depends on pH, amine buffer concentration, the nature of the amine buffer and pressure, but is independent of the concentration of Eu^{3+}. This step is attributed to the formation of the final 1:1 complex, Eu^{3+}–PAR^{2-}, shown above.

Kinetic studies of the first step

Eu^{3+} Concentration dependence. Table 1 presents the rate constants k_1 for the first step of the reaction of Eu^{3+} with PAR as a function of Eu^{3+} concentration either in a pH 2.08 succinate buffer or a pH 4.35 acetate buffer. The plots (Fig. 2) of k_1 *versus* $[Eu^{3+}]$ in both succinate and acetate buffers are linear with no significant intercept. The rate constants calculated from the slopes are 6.15×10^1 and 4.12×10^4 dm^3 mol^{-1} s^{-1} in succinate and acetate buffers, respectively. The large difference is attributed not only to the difference in pH but also to the nature of the buffers used (see **Effect of pH**). This kinetic behavior suggests that the first step follows the Eigen–Wilkins mechanism depicted in Scheme 2[69] where A represents H_2O, acetate or other buffer molecules which are involved in the co-ordination

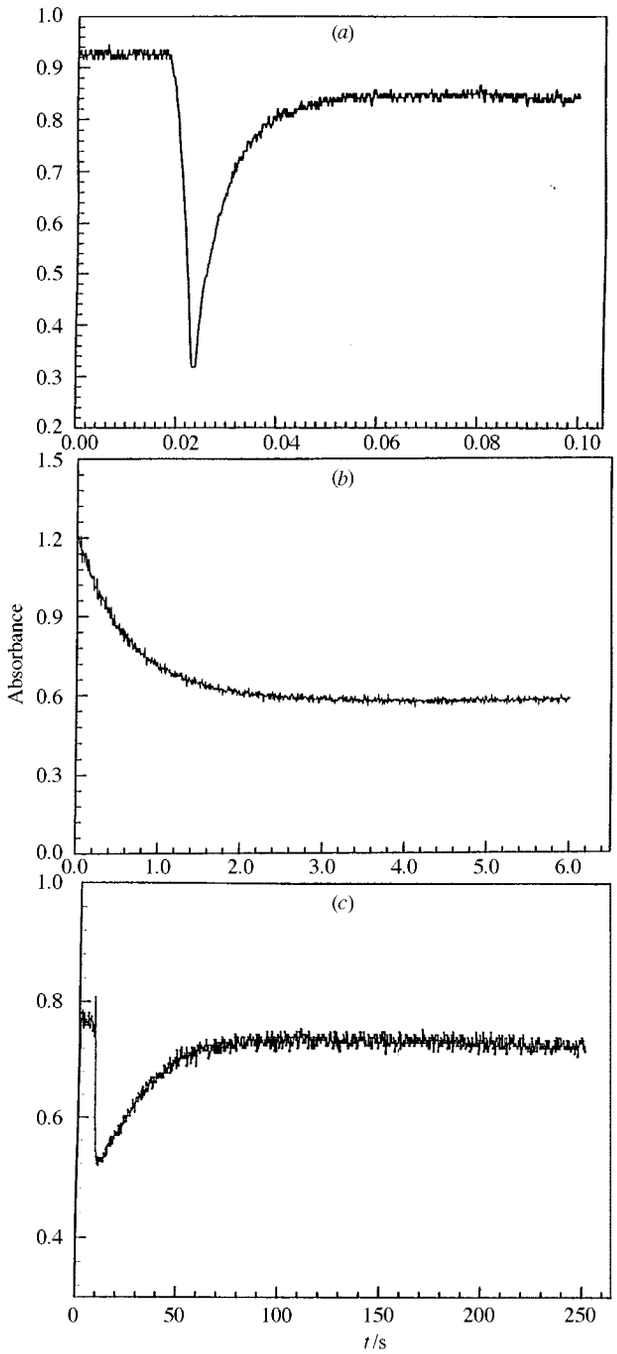

Fig. 1 Typical kinetic traces recorded for the first (a), second (b) and third step (c) of the reaction of Eu^{3+}(aq) with PAR at ambient pressure and 25.0 °C in 0.01 mol dm^{-3} HEPPS buffer solution (pH 7.55, $[Eu^{3+}] = 1 \times 10^{-3}$ mol dm^{-3}, $[PAR] = 1 \times 10^{-4}$ mol dm^{-3} and $[NaClO_4] = 0.1$ mol dm^{-3}).

to Eu^{3+}. From Scheme 2, d[product]/d$t = k_1$[b] but d[b]/d$t = -k_1$[b] $- k_{-1}''$[b] $+ k_1''$[a] $= 0$, [b] $= k_1''$[a]/$(k_1 + k_{-1}'')$ and d[product]/d$t = k_1k_1''$[a]/$(k_1 + k_{-1}'') = \{K_1'k_1k_1''$[Eu$(H_2O)_8(A)^{x+}$][PAR]$\}/(k_1 + k_{-1}'')$, but [PAR] $= K_{a1}$[H^+PAR]/[H^+]. Thus, d[product]/d$t = \{K_{a1}K_1'k_1k_1''$[Eu$(H_2O)_8$(A)$^{x+}$][H^+PAR]$\}/\{(k_1 + k_{-1}'')$[H^+]$\}$ where $K_1' = k_1'/k_{-1}'$. This rate law is consistent with the dependence on Eu^{3+} concentration shown in Table 1 and Fig. 2, and also agrees with the observed effect of pH discussed below.

Effect of pH. Measurements made in succinate and acetate buffer solutions covered the pH range 1.80–5.40. All runs were made at a constant ionic strength of $[NaClO_4] = 0.1$ mol dm^{-3} and a constant concentration of 0.05 mol dm^{-3} of the basic component of the buffer. Table 2 presents the observed rate

Table 1 Rate constants as a function of concentration of Eu^{3+} for the three steps of the reaction of Eu^{3+} (aq) with PAR at 25.0 °C and ambient pressure ([PAR] = 1×10^{-4} mol dm^{-3} and [$NaClO_4$] = 0.1 mol dm^{-3})

$[Eu^{3+}]$/mol dm^{-3}	$10k_1/s^{-1}$	$10k_2/s^{-1}$	$10k_3/s^{-1}$
pH 2.08 (succinate 0.05 mol dm^{-3})			
0.001	0.50 ± 0.02	3.90 ± 0.15	3.79 ± 0.09
0.002	1.42 ± 0.01	3.76 ± 0.09	3.58 ± 0.11
0.003	2.12 ± 0.13	3.68 ± 0.15	3.81 ± 0.12
0.004	2.53 ± 0.19	3.84 ± 0.10	3.72 ± 0.05
0.005	3.02 ± 0.14	3.59 ± 0.08	3.65 ± 0.11
pH 4.35 (acetate 0.05 mol dm^{-3})			
0.001	50 ± 3	10.1 ± 0.4	18.5 ± 0.4
0.002	89 ± 7	9.82 ± 0.2	19.0 ± 0.6
0.003	127 ± 6	9.53 ± 0.4	17.8 ± 0.6
0.005	204 ± 8	9.95 ± 0.3	18.9 ± 0.2
0.010	420 ± 12	9.30 ± 0.2	17.6 ± 0.5

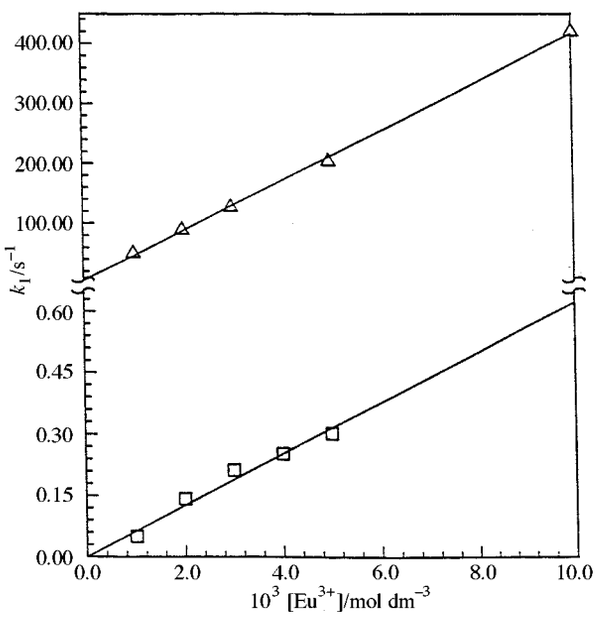

Fig. 2 Plots of k_1 *versus* Eu^{3+} concentration for the first step of the reaction of Eu^{3+} with PAR at ambient pressure and 25.0 °C ([Eu^{3+}] = 1×10^{-3} mol dm^{-3}, [PAR] = 1×10^{-4} mol dm^{-3} and [$NaClO_4$] = 0.1 mol dm^{-3}): △, pH 4.35, [acetate] = 0.05 mol dm^{-3}; □, pH 2.08, [succinate] = 0.05 mol dm^{-3}.

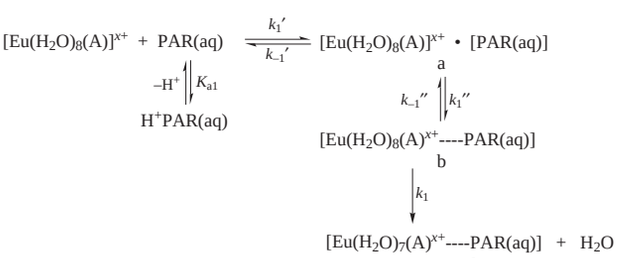

Scheme 2

constants as a function of pH in either succinate buffer or acetate buffer at ambient pressure and 25.0 °C. Fig. 3 is a linear plot of k_1 *versus* 1/[H^+] (k_1 increases with increasing 1/[H^+]) that proceeds through the origin in the succinate buffer in the pH range 1.80–3.31.

The rate constants of the first step in acetate buffered solution in the pH range 3.61–5.40 (see Table 2) are much faster, and are independent of the pH or 1/[H^+]. Although the acetate anion forms only weak complexes with lanthanide cations, for

Table 2 Rate constants as a function of pH for the first step of the reaction of Eu^{3+}(aq) with PAR *

pH	$10k_1/s^{-1}$
[succinate] = 0.05 mol dm^{-3}	
1.80	0.07 ± 0.06
2.08	0.83 ± 0.04
2.30	1.90 ± 0.16
2.65	5.00 ± 0.04
2.89	8.96 ± 0.13
3.31	21.2 ± 0.5
[acetate] = 0.05 mol dm^{-3}	
3.62	48.9 ± 1.3
4.14	50.2 ± 1.3
4.35	50.2 ± 1.8
4.58	48.5 ± 1.7
5.02	46.9 ± 1.1
5.40	49.6 ± 2.3

* Experimental conditions: [Eu^{3+}] = 1×10^{-3} mol dm^{-3}; [PAR] = 1×10^{-4} mol dm^{-3}; 25.0 °C; [$NaClO_4$] = 0.1 mol dm^{-3}.

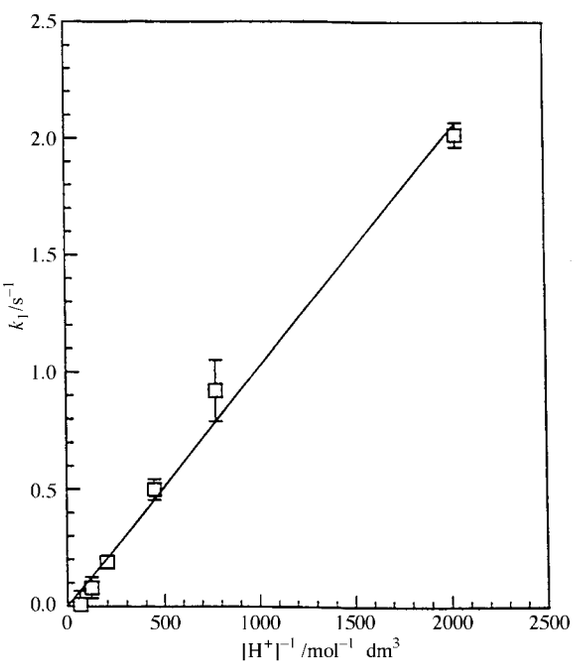

Fig. 3 Plot of k_1 *versus* $[H^+]^{-1}$ for the first step of the reaction of Eu^{3+} with PAR at ambient pressure and 25.0 °C in 0.05 mol dm^{-3} succinate buffered solution ([Eu^{3+}] = 1×10^{-3} mol dm^{-3}, [PAR] = 1×10^{-4} mol dm^{-3} and [$NaClO_4$] = 0.1 mol dm^{-3}).

example, log $\beta_1 \approx 1.9$ for $EuAc^{2+}$,[16] the concentration of acetate is very large compared with the other species present. Therefore, the Ac^- involvement in co-ordination must be considered. Calculations from the thermodynamic equilibrium data indicate that the concentration of $EuAc^{2+}$ is about 40% of that of Eu^{3+}(aq) in solutions of pH 4.5 when [HAc] + [Ac^-] ⩾ [Eu^{3+}].[70] Some kinetic studies[71–73] indicate that the catalytic effect results from a *trans* labilization effect by co-ordinated acetate and involves the attack by a solvent water molecule on the metal–carbon bond for the heterolysis reaction of (α-hydroxyalkyl)chromium(III). The co-ordinated acetate accelerates dissociation of water molecules from the inner co-ordination sphere of the metal ions, resulting in kinetic differences with reactions in unbuffered or other buffered solutions.[13,74] No protonated pyridine nitrogen exists in the acetate buffered pH range (3.61–5.40) since the pK_{a1} is as low as 2.35,[44] thus $[PAR]_{tot}$ = [PAR], and k_1 is independent of pH in acetate buffer.

Pressure dependence. The pressure dependence for the first

Table 3 Rate constants as a function of pressure for the three steps of the reaction of Eu^{3+}(aq) with PAR in different buffer solutions at 25.0 °C and $[Eu^{3+}] = 1 \times 10^{-3}$ mol dm^{-3} and $[NaClO_4] = 0.1$ mol dm^{-3}

	$10k_1$/s^{-1}			$\Delta V^{\ddagger}_1$/cm^3 mol^{-1}		
P/bar	pH 2.65 [succinate] = 0.05 [PAR] = 1×10^{-4}	pH 4.35 [acetate] = 0.05 [PAR] = 5×10^{-5}	pH 4.35 [acetate] = 0.05 [PAR] = 1×10^{-4}	pH 2.65 [succinate] = 0.05 [PAR] = 1×10^{-4}	pH 4.35 [acetate] = 0.05 [PAR] = 5×10^{-5}	pH 4.35 [acetate] = 0.05 [PAR] = 1×10^{-4}
1	0.50 ± 0.04	—	50.2 ± 1.8	+10.1 ± 0.7	+25.4 ± 3.8	+22.8 ± 0.56
50	0.49 ± 0.03	25.7 ± 1.4	47.3 ± 2.6			
250	0.44 ± 0.04	23.0 ± 2.3	40.0 ± 1.9			
500	0.40 ± 0.04	20.7 ± 0.4	32.7 ± 2.2			
750	0.36 ± 0.02	12.6 ± 0.4	25.0 ± 0.6			
1000	0.33 ± 0.02	10.1 ± 0.3	19.8 ± 1.4			
	k_2/s^{-1}	10^2k_3/s^{-1}		$\Delta V^{\ddagger}_2$/cm^3 mol^{-1}	$\Delta V^{\ddagger}_3$/cm^3 mol^{-1}	
P/bar	pH 4.35 [acetate] = 0.05 [PAR] = 1×10^{-4}	pH 4.35 [acetate] = 0.05 [PAR] = 1×10^{-4}	pH 7.10 [imidazole] = 0.05 [PAR] = 1×10^{-4}	pH 4.35 [acetate] = 0.05 [PAR] = 1×10^{-4}	pH 4.35 [acetate] = 0.05 [PAR] = 1×10^{-4}	pH 7.10 [imidazole] = 0.05 [PAR] = 1×10^{-4}
1	1.01 ± 0.08	1.85 ± 0.12	—	−15.9 ± 0.6	−11.2 ± 0.9	−15.9 ± 0.8
50	1.02 ± 0.11	1.92 ± 0.19	29.4 ± 2.5			
250	1.23 ± 0.07	2.25 ± 0.12	35.4 ± 2.0			
500	1.39 ± 0.12	2.40 ± 0.14	40.3 ± 3.4			
750	1.67 ± 0.05	2.70 ± 0.20	48.1 ± 3.5			
1000	1.91 ± 0.08	2.96 ± 0.24	55.3 ± 4.5			

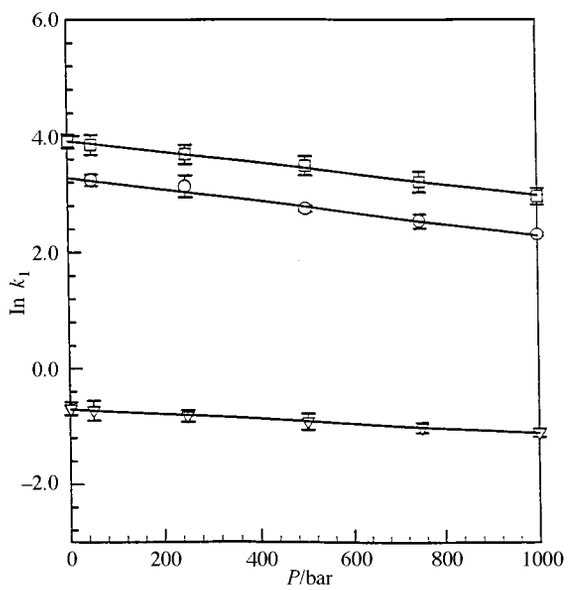

Fig. 4 Plots of ln k_1 *versus* pressure for the first step of the reaction of Eu^{3+} with PAR at 25.0 °C under different reaction conditions ($[Eu^{3+}] = 1 \times 10^{-3}$ mol dm^{-3} and $[NaClO_4] = 0.1$ mol dm^{-3}): □, pH 4.35, [PAR] = 1×10^{-4} mol dm^{-3}, [acetate] = 0.05 mol dm^{-3}; ○, pH 4.35, [PAR] = 5×10^{-5} mol dm^{-3}, [acetate] = 0.05 mol dm^{-3}; ▽, pH 2.66, [PAR] = 1×10^{-4} mol dm^{-3}, [succinate] = 0.05 mol dm^{-3}.

step of the reaction of Eu^{3+} with PAR was studied at different pH values, PAR concentrations and in different buffers at 25.0 °C. The k_1 values as a function of pressure under different reaction conditions are summarized in Table 3. Fig. 4 clearly shows a linear relationship between ln k_1 and pressure, from which it follows (see Table 3) that all $\Delta V^{\ddagger}_1$ values are positive. The $\Delta V^{\ddagger}_1$ values in acetate buffered solution (>+20 cm^3 mol^{-1}) are much larger than those found in succinate buffered solution (+10.1 cm^3 mol^{-1}). In general the pK_a values of buffers depend on pressure, typically for $HAc \rightleftharpoons H^+ + Ac^-$, $\Delta V \approx -12$ cm^3 mol^{-1}. It means that the buffer becomes more acidic (increase in K_a) with increasing pressure. In our system this will not affect the data in the acetate buffer since we found no pH dependence in this range. However, at lower pH in succinate buffer, a part of the observed $\Delta V^{\ddagger}_1$ could be due to the pressure dependence of the buffer, *i.e.* a lowering in pH due to an increase in K_a, which will slow down the reaction and show up as a positive $\Delta V^{\ddagger}$ value. These $\Delta V^{\ddagger}_1$ values demonstrate that when other reaction conditions are held constant the rate-determining step is the release of water molecules from the first co-ordination sphere. In succinate buffered solution an I_d mechanism apparently prevails, whereas in acetate buffered solution a D mechanism controls the first step because of the "acetate effect" mentioned above.

Influence of buffer. Since weak organic acids are frequently used as buffers, their ability to complex lanthanide cations should not be ignored. The stability constant, log β_n, of the lanthanide cation with the buffering anion increases with the pK_a of the buffer acid. Acetate buffer is a typical example. In neutral solutions buffers are often amine compounds. Complexation by these buffers may be of less concern. Thus our measurements of buffer concentration dependence were made in MES, HEPPS and Tris buffers over the 6.15–8.1 pH range. In this pH range the pyridinium ion of the ligand is completely dissociated (even in acetate buffer as discussed above). The rate of the first step is pH-independent and is subject to specific- and general-base catalysis so that $k_1 = k_0 + k_{OH}[OH^-] + k_b[B]$.

Fig. 5 shows typical plots of k_1 as a function of buffer base concentration. The linear plot for the MES buffers at pH 6.15 is evidence of general-base catalysis by this buffer when [MES] < 0.1 mol dm^{-3}. The non-linear plot of k_1 *vs.* [B$^-$] at pH 7.55 with HEPPS buffer suggests that specific interaction with this buffer obscures any base catalysis. The same phenomenon was observed by Reeves[55] for the complex formation of Ni^{II}-sulfonated 1-(2-pyridylazo)-2-naphthol (β-PAN) in HEPES buffer [*N*′-(2-hydroxyethyl)-*N*-piperazineethanesulfonic acid]. Reeves noted that absorption of β-PAN in a pH 6.89 HEPES buffer ([HEPES] = 0.01 mol dm^{-3}) in the absence of Ni^{II} has a significantly higher absorptivity than the curve for a MES buffer of the same pH and [B$^-$]. The interaction is apparently between the buffer and the dye and not with the metal ion. Similar evidence for a specific dye–buffer interaction between piperazine buffer and a cyano keto azo dye ligand has been observed.[60]

In the linear plot (Fig. 5) for the Tris buffer k_1 decreases with increasing Tris buffer concentration. This could be due to the multiple complexation equilibria between the buffer and Eu^{3+}.

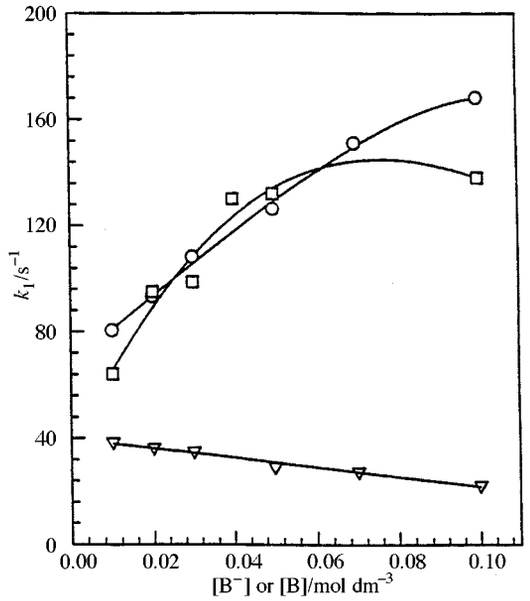

Fig. 5 Plot of the rate constant as a function of the concentration of buffer base in MES (○, pH 6.15), HEPPS (□, pH 7.55), and Tris (▽, pH 8.10) for the first step of the reaction of aqueous Eu^{3+} with PAR.

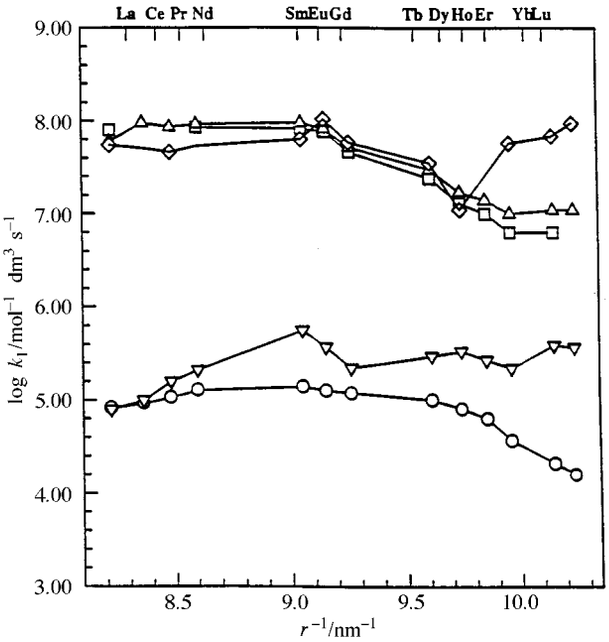

Fig. 6 Comparison of the complex-formation rate constants k_1 (second order rate constant) for some reactions of Ln^{3+} ions with different ligands in water, *versus* reciprocal metal ionic radius: ◇, L = anthranilate, see ref. 27; △, L = murexide, see refs. 25 and 26; □, L = oxalate, see ref. 29; ▽, L = CyDTA (cyclohexane-1,2-diyldinitrilotetraacetate), see ref. 31; ○, L = PAR, this work.

This kind of complexation between Ni^{II} and Tris has been reported.[75] The log β_1 for $Eu(Tris)^{3+}$ is *ca.* 2.5. For [Tris] = 0.005 mol dm^{-3}, [$EU(Tris)^{3+}$] would be 60% larger than [Eu^{3+}]. In addition, the formation of the hydrolysed europium species $Eu(OH)_n^{3-n}$, at such high pH causes a decrease in reactive europium concentration that cannot be neglected.

Different Ln^{3+}. The second order rate constants for the first step of the reaction of Ln^{3+} with PAR, k_1/dm^3 mol^{-1} s^{-1}, in logarithmic form, as a function of different lanthanide ions, and *versus* reciprocal metal ionic radius in 0.05 mol dm^{-3} MES buffer at pH 6.15, ambient pressure and 25.0 °C ([Ln^{3+}] = 1×10^{-3} mol dm^{-3}, [PAR] = 1×10^{-4} mol dm^{-3} and [$NaClO_4$] = 0.1 mol dm^{-3}), are given in Fig. 6. For comparison, the complex-formation rate constants of aqueous Ln^{3+} ions with some other ligands are also given in Fig. 6. The rates of complexation not only depend on the metal ion but also on the nature of the incoming ligand. The rate constants k_1 are seen to reach a maximum around samarium for our Ln^{3+}–PAR system. The same trends were observed for the complexations of lanthanide ions by sulfate,[22] acetate[23] and CyDTA.[30] Other workers[12,13,76,77] have concluded that there is probably a change in co-ordination number (CN) occurring from Sm^{3+} to Gd^{3+}. This may explain the observed change along the lanthanide series in the rate of almost all the complexations included in Fig. 6, as well as by sulfate and acetate. These results suggest a very easy substitution pathway for these ions, due to the almost identical energies of the octa- and nona-co-ordinated species. Moreover, the observation of an associative water-exchange[12] or complex-formation[13] mechanism on the octahydrated heavy Ln^{3+} ions (the smallest of the series according to their ionic radii) leads to the presumption of a larger co-ordination number for the lighter elements, thus reinforcing the idea of a co-ordination number change in the middle of the series.

The co-ordination numbers of the Ln^{3+} ions in water have been the subject of substantial debate,[78–80] but it is now established from neutron scattering,[76,81] X-ray scattering,[82] extended X-ray absorption fine structure (EXAFS),[5] density[83] and spectrophotometric[6] studies that the lighter La^{3+}–Nd^{3+} ions are predominantly nine-co-ordinate, Pm^{3+}–Gd^{3+} exist in equilibria between eight- and nine-co-ordinate states, and the heavier Tb^{3+}–Lu^{3+} are predominantly eight-co-ordinate.[5,6,76,81–83]

The systematic decrease in k_1 for L = PAR, oxalate and murexide shown in Fig. 6, and the decreasing water exchange rate,[12,84] as the ionic radius decreases from Gd^{3+} to Yb^{3+}, is consistent with increasing steric crowding, hindering the entry of the incoming ligand and dominating the variation of k_1. The corresponding increase in surface charge density might be expected to provide an increased electrostatic attraction between the entering ligand and Ln^{3+}, and thereby accelerate the co-ordination rate, but this is evidently not important here.

The k_1 values shown in Fig. 6, and the other rate constants of aqueous Ln^{3+} complexations by H_2O,[5,12] NO_3^-,[19,20] SO_4^{2-},[21,22] acetate,[23] picolinic acid,[24] methyl red,[26] malonate,[27] arsenazo III,[13] and acyclic aminopolycarboxylates, such as EDTA and DTPA,[18,29] vary by several orders of magnitude for the same metal ion. The ligands do not have the same steric properties and electronic charge and will have very different outer-sphere parameters. However, the difference in the k_1 values is probably due to various other factors as well, such as differences in experimental reaction conditions and measurement methods. It should also be recalled that the ligands in Fig. 6 are all weak bases, and competition may occur between protonation and metal bond formation on the ligand basic sites. This is exemplified by monoprotonated CyDTA complexation on the lanthanide ions where the complexation rate constants (≈3 dm^3 mol^{-1} s^{-1} at 25.0 °C) are governed by the final deprotonation step of the ligand.

In many studies[19–29] only one step was observed for the complexations of Ln^{3+} by various multidentate ligands on a short timescale because of limitations of the kinetic techniques, such as ultrasonic relaxation and NMR. Subsequent slower reaction steps were not observed. An advantage of the stopped-flow technique is the relatively slower accessible timescales permitting a more complete kinetic picture of the complexation of aqueous Ln^{3+} by multidentate ligands.

Based on the information given above, Scheme 3 provides a reasonable description of the first step of the complexation of aqueous Eu^{3+} by PAR in different buffered solutions.

Comparison between PAR and PAN. Owing to the low solubility of PAN in aqueous solution, a water–1,4-dioxane (3:1 v/v) mixed solvent was used to compare the kinetics of complexation of Eu^{3+}(aq) by PAN and PAR. The rate constant, k_1 (see

Table 4 Rate constants for the three steps of the complexation of Eu^{3+}(aq) by PAR or PAN in MES buffered, water–1,4-dioxane (3 : 1 v/v) at pH = 6.15, ambient pressure and 25.0 °C ($[Eu^{3}] = 1 \times 10^{-3}$ mol dm^{-3}, $[L] = 1 \times 10^{-4}$ mol dm^{-3} (L = PAR or PAN), [MES] = 0.05 mol dm^{-3} and $[NaClO_4] = 0.1$ mol dm^{-3})

L	λ_{max}/nm	k_1/s^{-1}	$10k_2/s^{-1}$	$10^2k_3/s^{-1}$
PAR	502	71.6 ± 0.90	1.85 ± 0.12	7.01 ± 0.73
PAN	532	5.89 ± 0.30	4.58 ± 0.12	1.01 ± 0.10

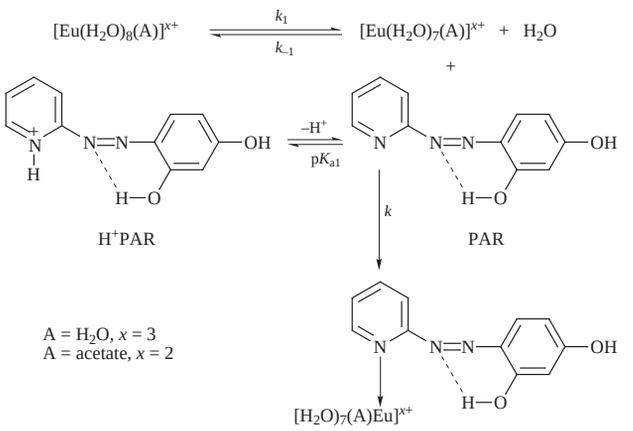

Scheme 3

Table 4), for the first step of the complexation of aqueous Eu^{3+} by PAR is 12 times greater than for PAN under the same reaction conditions. Scheme 1 shows that PAR exists as the monoanion PAR^- at pH 6.15 in MES buffer; PAN is a neutral molecule at the same pH. The negative charge on PAR gives rise to a higher electron density on the nitrogen atom of the pyridine moiety through conjugation. Consequently, the first complexation step takes place at a faster rate for PAR than for PAN.

In addition, the k_1 value (71.5 ± 0.9 s^{-1}) for PAR obtained in the water–1,4-dioxane mixed solvent is smaller than in pure water (126 ± 2 s^{-1}) under the same reaction conditions. Cusumano[61] also observed that rate constants for the complexation of nickel(II) by PAR and PAN in different non-aqueous solvents depend strongly on the nature of the solvent.

Comparison between Eu^{3+} and UO_2^{2+}. Although the number of actinide elements is the same as the number of lanthanide elements, the availability of the former and their chemical characteristics have so far largely restricted the study of their ligand substitution mechanisms to dioxouranium(VI), the ionic form of uranium most amenable to such studies in solution. Commonly observed solvated species have the stoichiometry $[UO_2(solvent)_5]^{2+}$, for example, $[UO_2(H_2O)_5]^{2+}$, characterized by two oxo ligands bound in axial sites with average axial U–O distances in the range 1.71–1.75 Å. Five water molecules occupying the equatorial plane have an average equatorial distance of 2.45 Å (see structure below). In solution the two oxo atoms undergo slow exchange, whereas the equatorial solvent molecules experience fast exchange. Thus the $[UO_2(solvent)_5]^{2+}$ system offers the opportunity to study solvent exchange in a single plane of a solvated metal ion.[2,85–87]

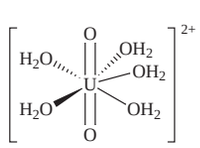

$UO_2(H_2O)_5^{2+}$

Kinetic data of the complexations of $UO_2(aq)^{2+}$ and Eu^{3+}(aq) by PAR in 0.1 mol dm^{-3} acetate buffer at pH 4.35 are summarized in Table 5. The k_1 value for the complexation of

Table 5 Rate constants for the three steps of the complexations of UO_2^{2+}(aq) and Eu^{3+}(aq) by PAR in acetate buffer at pH 4.35, ambient pressure and 25.0 °C ($[M] = 1 \times 10^{-3}$ mol dm^{-3}, M = UO_2^{2+} or Eu^{3+}; $[PAR] = 1 \times 10^{-4}$ mol dm^{-3}, [acetate] = 0.1 mol dm^{-3} and $[NaClO_4] = 0.1$ mol dm^{-3})

M	$10^{-1}k_1/s^{-1}$	k_2/s^{-1}	$10^2k_3/s^{-1}$
UO_2^{2+}	4.67 ± 0.10	0.94 ± 0.40	0.74 ± 0.50
Eu^{3+}	5.02 ± 0.18	1.00 ± 0.03	1.85 ± 0.11

UO_2^{2+} by PAR is about the same as that of the Eu^{3+}–PAR system. This suggests that the first step of the UO_2^{2+} complexation by PAR follows the same mechanism proposed for the lanthanides (see Schemes 2 and 3), even though there are two oxo ligands bound in the axial sites on UO_2^{2+}. Fux *et al.*[87] found that the rate constants of the observed first step of the complexation of UO_2^{2+} by 18-crown-6 and diazo-18-crown-6 in propylene carbonate are 930 ± 50 and 23 ± 1 s^{-1}, respectively. The mechanism is very similar to our mechanism proposed in Scheme 2. Comparing our rate constant k_1 with those found by Fux *et al.*[87] for reactions with UO_2^{2+}, we found that: k_1(18-crown-6, in propylene carbonate, 930 s^{-1}) > k_1(PAR, in water, 46.7 s^{-1}) > k_1(diazo-18-crown-6, in propylene carbonate, 23 s^{-1}). Our k_1 value is much closer to that for the complexation of UO_2^{2+} by the nitrogen atom in diazo-18-crown-6, which means that the complexation of UO_2^{2+} by an oxygen donor is faster and stronger than that by a nitrogen donor. This is attributed to the "hard acid" character of UO_2^{2+}.

Kinetic studies of the second step

In a typical kinetic trace shown in Fig. 1(b) for the observed second step the absorbance at 502 nm decreases with increasing time with a half-life of *ca.* 500 ms. Mochizuki *et al.*[88] observed a similar phenomenon in the complexation of Co^{2+} and Ni^{2+} by PAN in aqueous 1,4-dioxane. They proposed that the absorbance decrease is caused by the formation of the insoluble neutral intermediate $[Co^{II}(PAN^-)_2]^0$, and the slowest step, namely, the absorbance increase with increasing time is due to the formation of the soluble final product $[Co^{III}(PAN^-)_2]^+$. If the same process holds true for our Ln^{3+}–PAR (or PAN) system, the intermediates should be $[Ln^{II}(PAR^{2-})]^0$ or $[Ln^{II}(PAR^-)_2]^0$, and $[Ln^{II}(PAN^-)_2]^0$, respectively. However, if it is kept in mind that for our kinetic studies aqueous Ln^{3+} ions were always in excess concentration and only samarium, europium and ytterbium have +2 oxidation states,[70] it is obvious that the suggestion by Mochizuki *et al.*[88] cannot apply to our Ln^{3+}–PAR (or PAN) system. We propose that the formation of the "hydrazone–Ln^{3+} chelate" intermediate (see the structure below) is more reasonable because it destroys the whole conjugated structure which is the basis of many azo dyes. It therefore becomes interesting to explore whether the formation of a "hydrazone–M^{n+} chelate" intermediate is a common phenomenon during multi-step complexations of metal cations by many azo dyes.

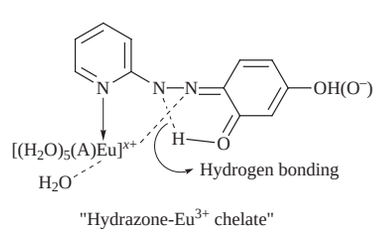

"Hydrazone-Eu^{3+} chelate"

Eu^{3+} Concentration dependence. The rate constants for the second step of the reaction of Eu^{3+} with PAR, k_2, as a function of Eu^{3+} concentration, either in a pH 2.08 succinate buffer or a pH 4.35 acetate buffer, are summarized in Table 1. One sees that k_2 is independent of Eu^{3+} concentration either in succinate

Table 6 Rate constants as a function of pH for the second step of the reaction of $Eu(aq)^{3+}$ with PAR in acetate buffer ([acetate] = 0.05 mol dm^{-3}) solution at ambient pressure and 25.0 °C ($[Eu^{3+}] = 1 \times 10^{-3}$ mol dm^{-3}, $[PAR] = 1 \times 10^{-4}$ mol dm^{-3} and $[NaClO_4] = 0.1$ mol dm^{-3})

pH	k_2/s^{-1}
3.62	1.01 ± 0.04
4.14	1.03 ± 0.03
4.35	1.00 ± 0.03
4.58	0.99 ± 0.05
5.02	0.96 ± 0.04
5.40	1.02 ± 0.05

or acetate buffers which suggests that "intramolecular ring closure" must be rate-determining.

pH Dependence. Measurements made in acetate buffer solutions covered the pH range 3.61–5.40. All runs were made at a constant ionic strength of $[NaClO_4] = 0.1$ mol dm^{-3} and a constant (0.05 mol dm^{-3}) concentration of the basic component of the buffer. The observed rate constants as a function of pH in acetate buffered solution at ambient pressure and 25.0 °C are shown in Table 6. The k_2 values are independent of pH. This result is consistent with the formation of a "hydrazone–Eu^{3+} chelate" intermediate proposed above which does not involve any deprotonation or acid–base equilibrium.

Pressure dependence. The pressure dependence for the second step of the reaction of Eu^{3+} with PAR was studied in 0.05 mol dm^{-3} acetate buffer at 25.0 °C (see Table 3). The plots of ln k_2 *versus* pressure yield a $\Delta V^{\ddagger}_2$ value -15.9 ± 0.6 cm^3 mol^{-1}. The negative sign suggests that the rate-determining process of the second step has an associative character. This result is also consistent with the intermediate formation of the "hydrazone–Eu^{3+} chelate" proposed above, which will involve a ring compact transition state.

Influence of buffer. The k_2 values as a function of buffer concentration in MES (pH 6.15), HEPPS (pH 7.55) and Tris (pH 8.10) buffers at ambient pressure and 25.0 °C over the concentration range of 0.01–0.10 mol dm^{-3} are given in SUP 57431. In all three buffers the rate constants are independent of buffer concentration. Absence of a buffer effect in this step suggests that the mechanism does not involve complex formation between the buffer and Eu^{3+} species. The k_2 values obtained from MES and HEPPS are very similar. On the other hand, the values obtained with Tris buffer (higher pH) are smaller. The difference is probably caused by a decrease in concentration of the reactive Eu^{3+} species at such a high pH (8.10) in the Tris buffer due to hydrolysis to form $Eu(OH)_n^{3-n}$ as mentioned before.

Comparison between PAR and PAN. Measurements were made under the same reaction conditions as for the first step except for the timescale. Table 4 indicates that the k_2 value (0.458 s^{-1}) for the complexation of Eu^{3+} by PAN is larger than that for PAR (0.185 s^{-1}). The extra benzene ring of the Eu^{3+}–PAN intermediate may make it more stable than the Eu^{3+}–PAR intermediate because of further conjugation.

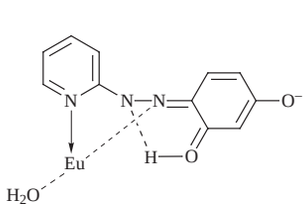

Eu^{3+}-PAR hydrazone chelate

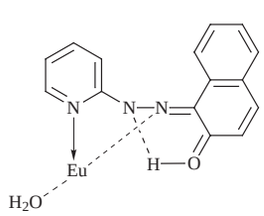

Eu^{3+}-PAN hydrazone chelate

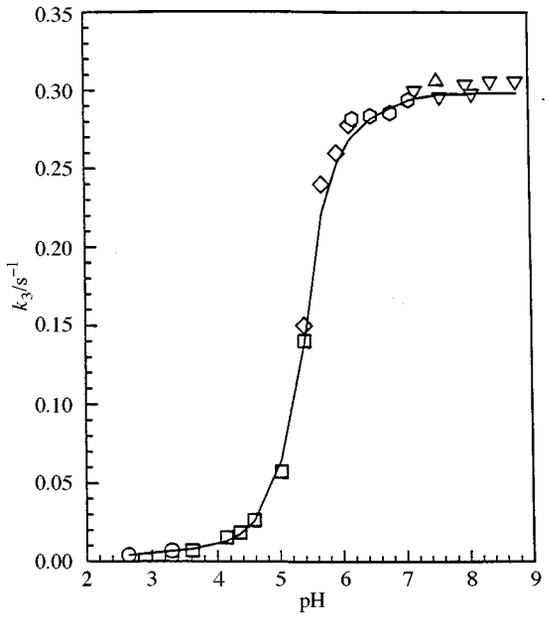

Fig. 7 Plot of k_3 *versus* pH for the third step of the reaction of Eu^{3+} with PAR at ambient pressure and 25.0 °C in different buffer solutions ($[Eu^{3+}] = 1 \times 10^{-3}$ mol dm^{-3}, $[PAR] = 1 \times 10^{-4}$ mol dm^{-3}, $[NaClO_4] = 0.1$ mol dm^{-3} and [buffer] = 0.05 mol dm^{-3}). Buffers: ○, succinate; □, acetate; △, HEPPS; ⬡, imidazole; ◇, MES; ▽, Tris.

Comparison between Eu^{3+} and UO_2^{2+}. Table 5 shows that the k_2 value for the complexation of UO_2^{2+} (0.94 s^{-1}) by PAR is about the same as that of the Eu^{3+}–PAR system (1.00 s^{-1}). This suggests that the second step of the UO_2^{2+} complexation by PAR follows the same pathway as for the lanthanides. Desolvation and formation of the "UO_2^{2+}–PAN hydrazone intermediate" must be completed within the equatorial plane. The two axial U=O bonds do not affect the complexing process. Again, it is interesting to compare our k_2 value for the complexation of UO_2^{2+} by PAR with observed rate constants for the complexation of uranyl ion by 18-crown-6 or diazo-18-crown-6.[86] Our k_2 value is close to that of the UO_2^{2+}–diazo-18-crown-6 system (1.3 s^{-1}) and smaller than that of the UO_2^{2+}–18-crown-6 system (18 s^{-1}). Fux *et al.*[87] proposed that the rate-determining rearrangement reaction in the UO_2L "external" complex consists of metal and ligand cavity desolvations with a simultaneous rotation of the uranyl group to give the UO_2L "exclusive" complex.

Different Ln^{3+}. Measurements were carried out under the same reaction conditions as for the first step except for the timescale. All the k_2 values for the complexation of the lanthanides from Sm^{3+} to Lu^{3+} by PAR are close to 2.0 s^{-1}, and parallel the stability constants for Ln^{3+}–PAR^-. The second step was not observed for the complexation of La^{3+}, Ce^{3+}, Pr^{3+} and Nd^{3+} by PAR. Our observations here are consistent with the work by Merbach and co-workers.[7–12,76,80,84,85]

Based on the above, the second step of the complexation of aqueous Eu^{3+} by PAR is adequately represented by Scheme 4.

Kinetic studies of the third step

pH and Eu^{3+} Concentration dependence. pH Dependence studies were carried out in succinate, acetate, imidazole, MES, HEPPS and Tris buffered solutions covering the pH range 1.80–8.80. All runs were made at a constant ionic strength of $[NaClO_4] = 0.1$ mol dm^{-3} and a constant 0.05 mol dm^{-3} concentration of the basic component of the buffer. The observed rate constants as a function of pH in all buffered solutions at ambient pressure and 25.0 °C are given in Table 7. Fig. 7 shows that a plot of k_3 *versus* pH has a typical "titration curve" from pH 4 to 7. This demonstrates that there must be a deprotonation

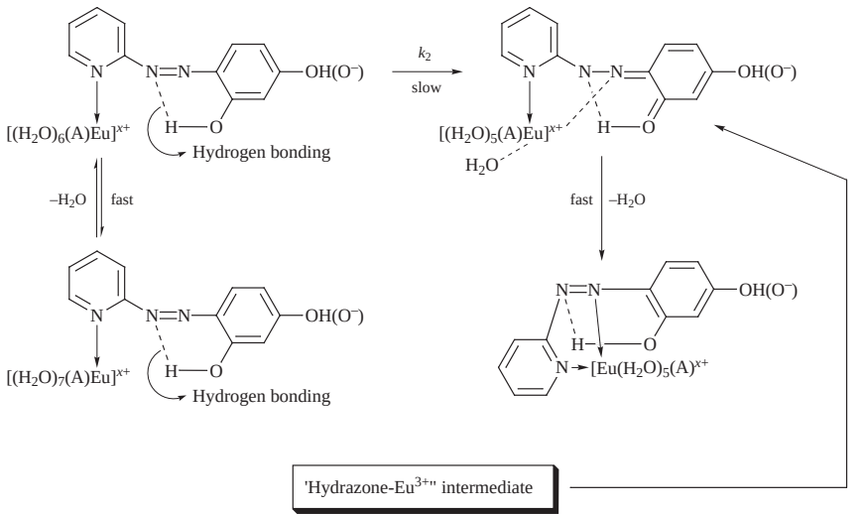

Scheme 4

Table 7 Rate constants as a function of pH for the third step of the reaction of aqueous Eu^{3+} with PAR in different buffer solutions at ambient pressure and 25.0 °C ($[Eu^{3+}] = 1 \times 10^{-3}$ mol dm^{-3}, [PAR] = 1×10^{-4} mol dm^{-3} and $[NaClO_4] = 0.1$ mol dm^{-3})

Buffer	pH	$10^2 k_3/s^{-1}$
Succinate	2.65	0.37 ± 0.02
	3.31	0.64 ± 0.03
Acetate	3.61	0.68 ± 0.03
	4.14	1.54 ± 0.09
	4.35	1.85 ± 0.11
	4.58	2.64 ± 0.18
	5.02	5.74 ± 0.27
	5.40	14.0 ± 0.9
MES	5.40	15.0 ± 1.2
	5.70	24.0 ± 1.2
	5.95	26.0 ± 0.2
	6.15	27.8 ± 2.2
Imidazole	6.21	28.2 ± 3.0
	6.50	28.4 ± 1.3
	6.81	28.6 ± 2.4
	7.10	29.4 ± 2.3
HEPPS	7.55	30.6 ± 2.7
Tris	7.20	30.0 ± 1.5
	7.60	29.6 ± 2.4
	8.00	30.4 ± 1.5
	8.10	29.8 ± 1.7
	8.40	30.6 ± 2.6
	8.80	30.6 ± 3.0

pre-equilibrium prior to the rate -determining step for the third step of the complexation of aqueous Eu^{3+} by PAR. The pre-equilibrium should be the deprotonation of *o*-hydroxyl with the hydrogen bonding shown. An approximate value of the pK_a for the pre-equilibrium, *i.e.* 5.4, can be deduced from the data of Table 7/Fig. 7. Rate constants k_3 for the third step of the reaction of Eu^{3+} with PAR as a function of Eu^{3+} concentration either in a pH 2.08 succinate buffer or a pH 4.35 acetate buffer are given in Table 1. They are seen to be independent of the Eu^{3+} concentration either in succinate or acetate buffers, which means that an "intramolecular rearrangement" or "intramolecular ring closure" is the rate-determining step.

Pressure dependence. The pressure dependence for the third step of the reaction of Eu^{3+} with PAR was studied either in 0.05 mol dm^{-3} acetate buffer at pH 4.35 or in 0.05 mol dm^{-3} imidazole buffer (pH 7.10) at 25.0 °C. The k_3 values as a function of

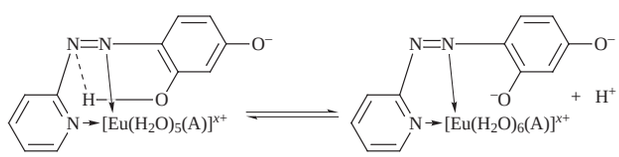

pressure are summarized in Table 3. The plots of ln k_3 *versus* pressure indicate that the $\Delta V^{\ddagger}_3$ value in 0.05 mol dm^{-3} acetate buffer at pH 4.35 is -11.2 ± 0.9 cm^3 mol^{-1} and the $\Delta V^{\ddagger}_3$ value in 0.05 mol dm^{-3} imidazole buffer at pH 7.10 is -15.9 ± 0.8 cm^3 mol^{-1}. These $\Delta V^{\ddagger}$ values suggest that the rate-determining process in the third step of the complexation, like the second step described above, is dominated by an associative character and a compact transition state.

Influence of buffer. The k_3 values as a function of buffer concentrations in MES (pH 6.15), HEPPS (pH 7.55) and Tris (pH 8.10) buffered solutions at ambient pressure and 25.0 °C over the concentration range of 0.01–0.10 mol dm^{-3} are given in SUP 57431. They show that in HEPPS and Tris buffers the observed rate constants for the third step of the complexation are independent of the concentrations of the buffers used. The absence of a buffer effect in the third step suggests that the mechanism does not involve complex formation between the buffers and "hydrazone–Eu^{3+} chelate" or the following "azo–Eu^{3+}, pseudo-phenanthroline style" chelate species. The k_3 values obtained in both HEPPS and Tris are very close. However, the k_3 values obtained from MES buffer (lower pH) decrease with increasing concentration of the MES buffer. We do not know the cause of this difference. Correlating with the pH-dependent studies shown in Fig. 7, we found that in MES buffered solution at pH 6.15 the k_3 value does not reach the saturation value. Probably, the higher the concentration of the MES buffer, the more difficult is the deprotonation of the *o*-hydroxyl because of intramolecular hydrogen bonding, and therefore the smaller are the k_3 values.

Different Ln^{3+}. Kinetic measurements were performed under the same reaction conditions as for the first and the second steps except for the timescale. All the k_3 values for the complexation of the lanthanides by PAR are close to 0.25 s^{-1}. Thus the third step of the complexation of aqueous Ln^{3+} by PAR is not affected by the nature of the lanthanide.

Comparison between PAR and PAN. Table 4 indicates that the k_3 value (0.01 s^{-1}) for the complexation of Eu^{3+} by PAN is smaller than that by PAR (0.07 s^{-1}). The two negative charges due to deprotonation of both the *o*- and *p*-hydroxyl groups of

PAR at pH 6.15 in MES buffer make the co-ordination by the *o*-oxyl anion of PAR^{2-} much easier than by PAN^{-} which has only one negative charge as a result of deprotonation. Therefore, the third step of the complexation of Eu^{3+} by PAR is faster than that of PAN.

Comparison between Eu^{3+} and UO_2^{2+}. Table 5 shows that the k_3 value for the complexation of UO_2^{2+} (0.0074 s^{-1}) by PAR is smaller than that of the Eu^{3+}–PAR system (0.0185 s^{-1}). This means that the third step for UO_2^{2+} complexation by PAR is slowed down by the two axial U=O bonds. In order to complete the slowest step, namely, the co-ordination of the UO_2^{2+}–PAR intermediate from the second step by the *o*-oxyl anion of PAR, the two axial U=O bonds must rotate to some degree. The formation of the transition state cannot be completed within the equatorial plane. The k_3 value of the UO_2^{2+}–PAR system is also smaller than that in the third observed step of the complexation of UO_2^{2+} by either 18-crown-6 (0.022 s^{-1}) or by diazo-18-crown-6 (0.283 s^{-1}).[87]

On the basis of the above kinetic results for the third step of the complexation of aqueous Eu^{3+} by PAR we propose the mechanism depicted in Scheme 5.

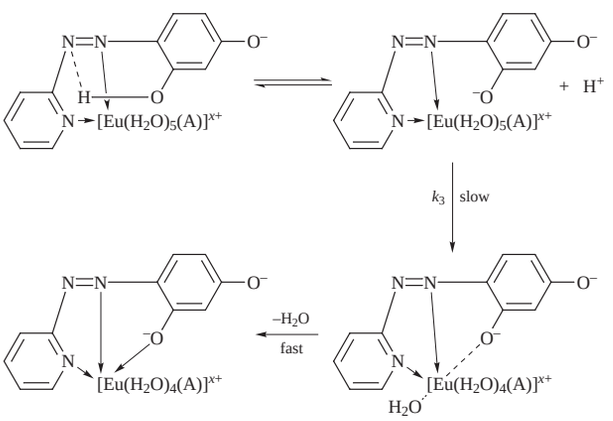

Scheme 5

Acknowledgements

Financial support by the Department of Energy, Office of Basic Energy Sciences (Y. S. and E. M. E.) and by the Volkswagen Foundation (R. v. E.) is gratefully acknowledged.

References

1 S. F. Lincoln, *Adv. Inorg. Bioinorg. Mech.*, 1983, **4**, 217.
2 S. F. Lincoln and A. E. Merbach, in *Advances in Inorganic Chemistry*, ed. A. G. Sykes, Academic Press, San Diego, 1995, vol. 42.
3 L. Helm and A. E. Merbach, *Eur. J. Solid State Inorg. Chem.*, 1991, **28**, 245.
4 A. Habenschuss and F. H. Spedding, *J. Chem. Phys.*, 1980, **73**, 442.
5 T. Yamaguchi, M. Nomura, H. Wakita and H. Ohtaki, *J. Chem. Phys.*, 1988, **89**, 5153.
6 K. Miyakawa, Y. Kaizu and H. Kobayashi, *J. Chem. Soc.*, *Faraday Trans.*, 1988, **84**, 1517.
7 N. Graeppi, D. H. Powell, G. Laurenczy, L. Zekány and A. E. Merbach, *Inorg. Chim. Acta*, 1995, **235**, 311.
8 C. Cossy, L. Helm and A. E. Merbach, *Inorg. Chem.*, 1988, **27**, 1973.
9 D. Pubanz, G. González, D. H. Powell and A. E. Merbach, *Inorg. Chem.*, 1995, **34**, 4447.
10 Th. Kowall, F. Foglia, L. Helm and A. E. Merbach, *J. Am. Chem. Soc.*, 1995, **117**, 3790.
11 K. Micskei, L. Helm, E. Brücher and A. E. Merbach, *Inorg. Chem.*, 1993, **32**, 3844.
12 C. Cossy, L. Helm and A. E. Merbach, *Inorg. Chem.*, 1989, **28**, 2699.
13 Y. Shi, E. M. Eyring and R. van Eldik, *J. Chem. Soc.*, *Dalton Trans.*, 1998, 967.
14 R. B. Lauffer, *Chem. Rev.*, 1987, **87**, 901.
15 S. Jurisson, D. Berning, W. Jia and D. Ma, *Chem. Rev.*, 1993, **93**, 1137.
16 M. F. Tweedle, in *Lanthanide Probes in Life*, *Chemical and Earth Sciences*: *Theory and Practices*, eds. J.-C. G. Bünzli and G. R. Choppin, Elsevier, Amsterdam, 1989.
17 V. Alexander, *Chem. Rev.*, 1995, **95**, 273.
18 G. R. Choppin and P. J. Wong, *ACS Symp. Ser.*, 1994, **565.**
19 H. B. Silber, N. Scheinin, G. Atkinson and J. Grecsek, *J. Chem. Soc.*, *Faraday Trans.*, 1972, **68**, 1200.
20 R. Garnsey and D. W. Ebdon, *J. Am. Chem. Soc.*, 1969, **91**, 50.
21 N. Purdie and C. A. Vincent, *Trans. Faraday*, *Soc.*, 1967, **63**, 2745.
22 D. P. Fay, D. Litchinsky and N. Ourdie, *J. Phys. Chem.*, 1969, **73**, 544.
23 T. E. Eriksen, I. Grenthe and I. Puigdomenech, *Inorg. Chim. Acta*, 1987, **126**, 131.
24 M. M. Farrow, N. Purdie and E. M. Eyring, *Inorg. Chem.*, 1974, **13**, 2024.
25 T. E. Eriksen, I. Grenthe and I. Puigdomenech, *Inorg. Chim. Acta*, 1986, **121**, 63.
26 H. B. Silber, R. D. Farina and J. H. Swinehart, *Inorg. Chem.*, 1969, **8**, 819.
27 M. M. Farrow and N. Purdie, *Inorg. Chem.*, 1974, **13**, 2111.
28 A. J. Graffeo and J. L. Bear, *J. Inorg. Nucl. Chem.*, 1968, **30**, 1577.
29 G. R. Choppin, *J. Alloys Compd.*, 1995, **225**, 242.
30 G. A. Nyssen and D. W. Margerum, *Inorg. Chem.*, 1970, **9**, 1814.
31 K. Kumar, T. Jin, X. Wang, J. F. Desreus and M. F. Tweedle, *Inorg. Chem.*, 1994, **33**, 3823.
32 É. Tóth, E. Brücher, I. Lázár and I. Tóth, *Inorg. Chem.*, 1994, **33**, 4070.
33 K. Kumar and M. F. Tweedle, *Inorg. Chem.*, 1993, **32**, 4193.
34 E. Brücher, S. Cortes, F. Chavez and A. D. Sherry, *Inorg. Chem.*, 1991, **30**, 2092.
35 M. Kodama, T. Koike, A. B. Mahatma and E. Kimura, *Inorg. Chem.*, 1991, **30**, 1270.
36 K.-Y. Choi, K. S. Kim and J. C. Kim, *Polyhedron*, 1994, **13**, 567.
37 E. Brücher and A. D. Sherry, *Inorg. Chem.*, 1990, **29**, 1555.
38 K. Kumar, C. A. Chang and M. F. Tweedle, *Inorg. Chem.*, 1993, **32**, 587.
39 C. A. Chang, H.-L. Peter, V. K. Manchanda and S. P. Kasprzyk, *Inorg. Chem.*, 1988, **27**, 3786.
40 J. Geoges, *Spectrochim. Acta Rev.*, 1991, **14**, 337.
41 D. Betteridge and D. Hohn, *Analyst* (*London*), 1973, **98**, 377.
42 I. M. Rao, D. Satyanarayana and U. Agarwala, *Bull. Chem. Soc. Jpn.*, 1979, **52**, 588.
43 P. M. Drozdzewski, *Spectrochim. Acta*, *Part A*, 1985, **41**, 1035.
44 W. J. Geary, G. Nickless and F. H. Pollard, *Anal. Chim. Acta*, 1962, **26**, 575.
45 F. Zhao, Y. Liang, Y. Zhang and D. Tong, *Chin. Chem. Lett.*, 1992, **3**, 107.
46 A. Corsini, I. M. Yih, Q. Fernando and H. Freiser, *Anal. Chem.*, 1962, **34**, 1090.
47 A. Corsini, Q. Fernando and H. Freiser, *Inorg. Chem.*, 1963, **2**, 224.
48 H. J. Méndez, B. M. Cordero, J. L. Pavón and J. C. Miralles, *Inorg. Chim. Acta*, 1987, **140**, 245.
49 A. Cladera, E. Gómez, J. M. Estela and V. Cerdà, *Anal. Chem.*, 1993, **65**, 707.
50 K. Ueda, H. Matsuda and O. Yoshimura, *Anal. Sci.*, 1989, **5**, 725.
51 E. Ohyoshi, *Talanta*, 1984, **31**, 1129.
52 E. Ohyoshi, *Anal. Chem.*, 1983, **55**, 2404.
53 M. Tanaka, S. Funahashi and K. Shirai, *Anal. Chim. Acta*, 1967, **39**, 437.
54 B. Perlmutter-Hayman and R. Shinar, *Inorg. Chem.*, 1976, **15**, 2932.
55 R. L. Reeves, *Inorg. Chem.*, 1986, **25**, 1473.
56 R. H. Hoyler, C. D. Hubbard, S. F. A. Kettle and R. G. Wilkins, *Inorg. Chem.*, 1966, **5**, 622.
57 R. L. Reeves, G. S. Calabrese and S. A. Harkaway, *Inorg. Chem.*, 1983, **25**, 3076.
58 E. Mentasti and C. Baiocchi, *J. Chem. Soc.*, *Dalton Trans.*, 1985, 2615.
59 H. L. Fritz and J. H. Swinehart, *Inorg. Chem.*, 1975, **14**, 1935.
60 G. Meyers, F. M. Michaels, R. L. Reeves and P. P. Trotter, *Inorg. Chem.*, 1985, **24**, 731.
61 M. Cusumano, *Inorg. Chim. Acta*, 1977, **25**, 207.
62 S. Funahashi and M. Tanaka, *Inorg. Chem.*, 1969, **8**, 2159.
63 C. D. Hubbard and A. D. Pacheco, *J. Inorg. Nucl. Chem.*, 1977, **39**, 1373.
64 C. F. Shaw III, J. E. Laib, M. M. Savas and D. H. Petering, *Inorg. Chem.*, 1990, **29**, 403.
65 S. Funahashi and M. Tanaka, *Bull. Chem. Soc. Jpn.*, 1976, **49**, 2481.
66 H. Wada and G. Nakagawa, *Bull. Chem. Soc. Jpn.*, 1979, **52**, 3559.
67 R. Van Eldik, W. Gaede, S. Wieland, J. Kraft, M. Spitzer and D. A. Palmer, *Rev. Sci. Instrum.*, 1993, **34**, 1355.

68 H. Hoshino, T. Yotsuyanagi and K. Aomura, *Anal. Chim. Acta*, 1976, **83**, 317.
69 M. Eigen and R. G. Wilkins, *Adv. Chem. Ser.*, 1965, **49**, 55.
70 G. R. Choppin, in *Lanthanide Probes in Life*, *Chemical and Earth Sciences*: *Theory and Practices*, eds. J.-C. G. Bünzli and G. R. Choppin, Elsevier, Amsterdam, 1989.
71 H. Cohen, W. Gaede, A. Gerhard, D. Meyerstein and R. van Eldik, *Inorg. Chem.*, 1992, **31**, 3805.
72 W. Gaede, R. van Eldik, H. Cohen and D. Meyerstein, *Inorg. Chem.*, 1993, **32**, 1997.
73 W. Gaede, A. Gerhard, R. van Eldik, H. Cohen and D. Meyerstein, *J. Chem. Soc.*, *Dalton Trans.*, 1992, 2065.
74 T. Shi and L. I. Elding, *Inorg. Chem.*, 1996, **35**, 735.
75 K. S. Bai and A. E. Martell, *J. Inorg. Nucl. Chem.*, 1969, **31**, 1697.
76 C. Cossy, A. C. Barnes, A. E. Merbach and J. Enderby, *J. Chem. Phys.*, 1989, **90**, 3254.
77 K. Miyakawa, Y. Kaizu and H. Kobayashi, *J. Chem. Soc.*, *Faraday Trans.*, 1988, **90**, 3254.
78 T. W. Swaddle, *Adv. Inorg. Bioinorg. Mech.*, 1983, **2**, 95.
79 S. F. Lincoln, *Adv. Inorg. Bioinorganic. Mech.*, 1986, **4**, 217.
80 C. Cossy and A. E. Merbach, *Pure. Appl. Chem.*, 1988, **60**, 1785.
81 L. Helm and A. E. Merbach, *Eur. J. Solid State Inorg. Chem.*, 1991, **28**, 245.
82 A. J. Habenschuss and F. H. Spedding, *J. Chem. Phys.*, 1980, **73**, 442.
83 F. Spedding, L. E. Shiers, M. A. Brown, J. L. Derer, D. L. Swanson and A. J. Habenschuss, *J. Chem. Eng. Data*, 1975, **20**, 81.
84 K. Micskei, D. H. Powell, L. Helm, E. Brücher and A. E. Merbach, *Magn. Reson. Chem.*, 1993, **31**, 1011.
85 A. Abou-Hamdan, N. Burki, S. F. Lincoln, A. E. Merbach and S. J. F. Vincent, *Inorg. Chim. Acta*, 1993, **207**, 27.
86 G. L. Honan, S. F. Lincoln and E. H. Williams, *J. Chem. Soc.*, *Dalton Trans.*, 1979, 320.
87 P. Fux, J. Lagrange and P. Lagrange, *J. Am. Chem. Soc.*, 1985, **107**, 5927.
88 K. Mochizuki, T. Imamura, T. Ito and M. Fujimoto, *Chem. Lett.*, 1977, 1239.

Paper 8/05808C